A Theoretical and Diagnostic Study of Solitary Waves and Atmospheric Blocking

N. BUTCHART

U.K. Meteorological Office, Bracknell, Berkshire, England

K. HAINES AND J. C. MARSHALL

Imperial College, London, England

(Manuscript received 21 July 1988, in final form 24 November 1988)

ABSTRACT

Theories which associate atmospheric blocking with isolated "free mode" solutions of the equations of motion are reviewed and the central role played by the potential function $\Lambda \equiv dq/d\psi$ (where q is the quasi-geostrophic potential vorticity and ψ is the streamfunction) is emphasized. This function provides the common dynamical link that draws together the weakly nonlinear (soliton) and fully nonlinear (modon) theories of isolated coherent structures.

A diagnostic study of the European blocking episode during October 1987 is presented and the relationship between q and ψ investigated by plotting scatter diagrams of quasi-geostrophic potential vorticity against the streamfunction on an isobaric surface. An approximate functional relationship is found allowing Λ to be defined. Over the blocking region, points on the scatter plot cluster around a straight line which is more steeply sloping than the straight line defined by points from nonblocking regions, demonstrating that the block exhibits a local minimum in Λ. Such a signature is characteristic of local fully nonlinear free mode structures, the prototype of which has been termed the "equivalent barotropic modon." The data strongly suggest that blocking episodes can exhibit local free-mode dynamics and that their persistence may in part be attributed to the robustness and stationary nature of these local coherent structures.

1. Introduction

The association between atmospheric blocking and certain localized solutions of the inviscid equations of motion called modons has been considerably strengthened by recent theoretical and observational studies which suggest that such structures can be excited by plausible forcing mechanisms. For example, the studies of Pierrehumbert and Malguzzi (1984) and Haines and Marshall (1987, hereafter referred to as HM) suggest that the atmosphere may permit a nonlinear resonance in which forcing by synoptic scale eddies can excite and/or reinforce a local nonlinear free mode, the prototype of which is the equivalent barotropic β-plane modon considered by McWilliams (1980) and its extension to the sphere by Verkley (1984, 1987). The interaction of barotropic eddies with a modon stationary in a zonal flow can, through an eddy straining mechanism first studied by Shutts (1983), induce potential vorticity transports which capture many of the essential details of the observations presented by Illari and Marshall (1983), Illari (1984), Hoskins et al. (1985) and Shutts (1986). In a complementary series of studies, Malguzzi and Malanotte-Rizzoli (1984, 1985, hereafter referred to as MR84 and MR85, respectively) investigate weakly nonlinear Rossby waves as idealized blocking models and again invoke an eddy forcing mechanism to maintain them.

Although the existence and known robustness of these analytical structures make them natural blocking candidates, the only quantitative evaluation of the relevance of modon theories to blocking, that due to McWilliams (1980), was inconclusive. The modon "existence condition" that excludes stationary Rossby waves in the far field was found by McWilliams to be only marginally satisfied, if at all, during the blocking episode over northern Europe in January 1963. Indeed some investigators have expressed the view that the very inability of modons to coexist with stationary Rossby waves within the analytical framework implies that their dynamics is irrelevant to blocking. However, HM have shown that equivalent barotropic coherent dipoles can exist on blocking time scales despite interactions with stationary Rossby waves which are excited in their lee. On a time scale of some 10 to 20 days the coherent structure generates Rossby lee waves which extract energy from the local coherent flow. Subsequent studies have recently demonstrated that these "radiating modons" are also relevant in a baroclinic frame-

Corresponding author address: Dr. K. Haines, Center for Meteorology and Physical Oceanography, Dept. of Earth, Atmospheric and Planetary Sciences, Massachusetts Institute of Technology, Cambridge, MA 02139.

work. Thus it does not seem fruitful to seek strict adherence to the "existence condition", which in any case can only be easily satisfied in an equivalent barotropic framework and is difficult to attain in a fully baroclinic atmosphere. Instead, in this study we seek a signature in the observations which is characteristic of all localized structures whether of the modon or the weakly nonlinear variety. In order that a structure be localized the flow must be configured in such a way that the "potential function" $\Lambda \equiv dq/d\psi$ has a local minimum, where q is the quasi-geostrophic potential vorticity and ψ is an appropriate streamfunction for the flow. In the analytical modon this minimum is ensured by choosing different functional relationships between q and ψ on open and closed streamlines, such that Λ is more negative inside the structure than the ambient Λ of the far field. (For a review of the dynamics of isolated structures, see Flierl 1987.)

In section 2 we present the dynamical background which is common to the strongly nonlinear and weakly nonlinear manifestations of isolated structures, highlighting the important role of the function Λ in determining their form. We particularly emphasize common aspects and attempt to draw together the weakly nonlinear approach of MR84 and the fully nonlinear modon theories. Section 3 presents scatter diagrams of potential vorticity against streamfunction during the European blocking episode of October 1987. This diagnostic demonstrates the existence of an approximate functional relationship between q and ψ and clearly shows that, within the blocking region, the implied function Λ takes the form of a "potential well," which acts to stabilize the block and encourages its maintenance by focusing and trapping the eddy activity associated with the traveling weather systems. Section 4 discusses the implications of the study for our understanding of blocking mechanisms.

2. The dynamics of isolated structures

Here the dynamics of isolated structures is considered, concentrating particularly on the context of atmospheric blocking. Emphasis is placed on the central role played by a potential function in determining the structure of both the weakly and strongly nonlinear solitary eddies. It is argued that the existence and form of this potential function can provide a useful indicator of the presence of solitary eddies in the atmosphere. The quasi-geostrophic framework is adopted for analytical convenience. Consider stationary flows satisfying the unforced, undamped quasi-geostrophic potential vorticity equation on an infinite midlatitude β-plane

$$J(\psi, q) = 0 \tag{1}$$

where ψ is the streamfunction and, using pressure, p, as the vertical coordinate

$$q \equiv \nabla^2\psi + \beta y + f_0{}^2 \frac{\partial}{\partial p}\left(\frac{1}{\sigma_{\text{ref}}}\frac{\partial \psi}{\partial p}\right)$$

is the potential vorticity. We use f_0 is a constant midlatitude value of the Coriolis parameter,

$$\sigma_{\text{ref}} = -\frac{1}{\rho\theta_{\text{ref}}}\frac{d\theta_{\text{ref}}}{dp}$$

is the static stability and $\theta_{\text{ref}}(p)$ is a reference potential temperature distribution. The Jacobian is given by

$$J(a, b) = \frac{\partial a}{\partial x}\frac{\partial b}{\partial y} - \frac{\partial a}{\partial y}\frac{\partial b}{\partial x}$$

where x is east, y is north.

Separating the flow into far fields, ψ_0, q_0 representing a zonal flow, and eddy components, ψ_1, q_1 we have

$$\left.\begin{aligned} \psi &= \psi_0(y, p) + \psi_1 \\ q &= q_0(y, p) + q_1 \end{aligned}\right\} \tag{2}$$

where

$$q_0 \equiv \psi_{0_{yy}} + \beta y + f_0{}^2 \frac{\partial}{\partial p}\left(\frac{1}{\sigma_{\text{ref}}}\frac{\partial \psi_0}{\partial p}\right)$$

$$q_1 \equiv \nabla^2\psi_1 + f_0{}^2 \frac{\partial}{\partial p}\left(\frac{1}{\sigma_{\text{ref}}}\frac{\partial \psi_1}{\partial p}\right).$$

Solutions to Eq. (1) are sought which are spatially isolated and satisfy the boundary conditions

$$\psi_1 \to 0 \quad \text{as} \quad |x|, |y| \to \infty \quad \text{and} \quad p \to 0 \tag{3a}$$

$$\frac{Dp}{Dt} = 0 \quad \text{at} \quad p = p_s, \tag{3b}$$

where p_s is the surface pressure (assumed constant). Substituting Eq. (2) into (1) gives

$$J(\psi_0, q_1) + J(\psi_1, q_0) + J(\psi_1, q_1) = 0. \tag{4}$$

Introducing the function Λ_0 associated with the basic state zonal flow

$$\Lambda_0(y, p) \equiv \left.\frac{dq_0}{d\psi_0}\right|_{\text{p const}} = -\frac{1}{U_0}\frac{\partial q_0}{\partial y},$$

Eq. (4) can be written

$$J(\psi_0, q_1 - \Lambda_0\psi_1) + J(\psi_1, q_1) = 0. \tag{5}$$

Equation (5) will form the basis of our discussion of isolated structures. The function $\Lambda_0(y, p)$ has often appeared in the literature in association with the refractive index of the basic state zonal flow (e.g., Matsuno 1970). It is important in wave propagation diagnostics such as the Eliassen-Palm flux as discussed, for example, by Butchart et al. (1982) and in the ray tracing studies of, for example, Hoskins and Karoly (1981). However, in the present study we are concerned with localized steady solutions; in this context an analogy can be drawn between the function Λ and the trapping potential, which may appear in the Schrö-

dinger equation confining an elementary particle, as shown below.

a. Weakly nonlinear waves

Most analytical studies of solitary eddies are based upon weakly nonlinear theory: see in particular MR84 for blocking applications. This approach will be considered carefully since it introduces ideas which can be usefully extended to the treatment of the strongly nonlinear eddies considered later. Small amplitude solutions to Eq. (5) are sought such that $\psi_1, q_1 \to \epsilon\tilde{\psi}_1, \epsilon\tilde{q}_1$ where $\epsilon \ll 1$ and $\tilde{\psi}_1, \tilde{q}_1 \approx O(1)$. Then the second term in Eq. (5), which is nonlinear in the perturbation fields, can be neglected to give at first order in ϵ:

$$J(\psi_0, \tilde{q}_1 - \Lambda_0\tilde{\psi}_1) = 0$$

which is satisfied if:

$$\tilde{q}_1 - \Lambda_0\tilde{\psi}_1 = 0. \tag{6}$$

Note that only the function Λ_0 associated with the far field zonal flow plays a role in determining the spatial form of the perturbation suggesting that, since $\Lambda_0 = \Lambda_0(y, p)$, it may be useful to separate the variables as follows:

$$\tilde{\psi}_1 = A(x)\phi(y, p)$$

$$\tilde{q}_1 = \phi A_{xx} + A\phi_{yy} + Af_0^2 \frac{\partial}{\partial p}\left(\frac{1}{\sigma_{\text{ref}}}\frac{\partial \phi}{\partial p}\right)$$

Equation (6) reduces to

$$\left.\begin{aligned} \phi_{yy} + f_0^2 \frac{\partial}{\partial p}\left(\frac{1}{\sigma_{\text{ref}}}\frac{\partial \phi}{\partial p}\right) + (\lambda - \Lambda_0)\phi = 0 \quad \text{(a)} \\ A_{xx} = \lambda A \quad \text{(b)} \end{aligned}\right\} \tag{7}$$

where λ is the constant of separation. The bottom boundary condition (3b) reduces to

$$\frac{\phi_p}{\phi} = \frac{U_{0_p}}{U_0} \quad \text{at} \quad p = p_s.$$

Equation (7) clearly demonstrates the role of the function Λ_0 in setting the meridional and vertical structure of the perturbation. It takes the form of an eigenvalue problem similar to the time-independent Schrödinger equation in which Λ_0 is the potential. If the perturbation is to be localized in the y and p directions, Λ_0 must have a minimum thus forming a "potential well." If this condition is met there will be a finite number of discrete eigenvalues λ, each associated with a trapped perturbation which is evanescent as $|y| \to \infty$ or $p \to 0$. This is consistent with the refractive index interpretation: waves are refracted away from regions of high Λ_0 and may therefore become trapped in a region of low Λ_0, the potential well. However, Λ_0 cannot trap the anomaly in the zonal direction. In solitary wave theory weak nonlinearities are invoked to confine the perturbation in the x direction.

Equation (7b) is dispersive and cannot support isolated structures except in the presence of a boundary. However, it is well known (e.g., Whitham 1974, p. 467; or Redekopp 1977) that for perturbations with a zonal long-wave scale such that $x = X/\sqrt{\epsilon}$ and for appropriate eigensolutions to Eq. (7a) such that $\lambda = \epsilon K$ [where X and K are O(1)], Eq. (7b) acquires an additional nonlinear term at the lowest order in ϵ. This term arises from the scaling of $J(\psi_1, q_1)$ in Eq. (5); see MR84, who show that Eq. (7b) becomes:

$$A_{XX} - KA + \frac{\delta}{2}A^2 = 0 \tag{8}$$

where δ is a constant obtained by multiplying Eq. (7a) by ϕ and integrating over y and p. This equation is the steady form of the Korteweg de-Vries (KdV) equation which, if K (i.e., λ) is positive, possesses localized solutions of the form:

$$A = \frac{3K}{\delta}\,\text{sech}^2\left(\frac{\sqrt{K}}{2}X\right). \tag{9}$$

The requirement of positive λ implies that the potential Λ_0 must also become positive in the far field if the solution is to be isolated in all directions. Much has been written about the properties of the KdV equation and its close relatives (for example, Malanotte-Rizzoli (1982) reviews some geophysical fluid applications). However, a useful conceptual interpretation of Eq. (8) can be made if it is expressed in the form:

$$A_{XX} + \left[(-K) - \left(-\frac{\delta A}{2}\right)\right]A = 0.$$

The KdV equation, when written in this way, can be seen to have much the same form as Eq. (7a) but now the solution itself, A, determines the spatial variation of the potential. It is clear from the form of the solution, Eq. (9), that this potential $(-\delta A/2)$ will always exhibit a trapping minimum. This self-interaction property whereby the anomaly provides its own potential well is another manifestation of the process by which nonlinearity balances dispersion, allowing the solitary eddy to remain steady. The interpretation in terms of a trapping potential is useful because it emphasizes that a similar process is at work confining the waves in the x direction as is operating in the y and p directions. We discuss later how this interpretation may be extended to the treatment of strongly nonlinear structures, thus unifying the two approaches to isolated eddies.

Malguzzi and Malanotte-Rizzoli (1984) use a weakly nonlinear approach to obtain solitary waves which resemble blocking anomalies. Figure 1 shows their mean flow trapping potential (actually $\frac{1}{4} + \Lambda_0(y, z)$, using z as vertical coordinate). Using this potential a trapped solution is obtained with $\lambda = 0.22$ (satisfying the small, positive requirement) which corresponds to an equiv-

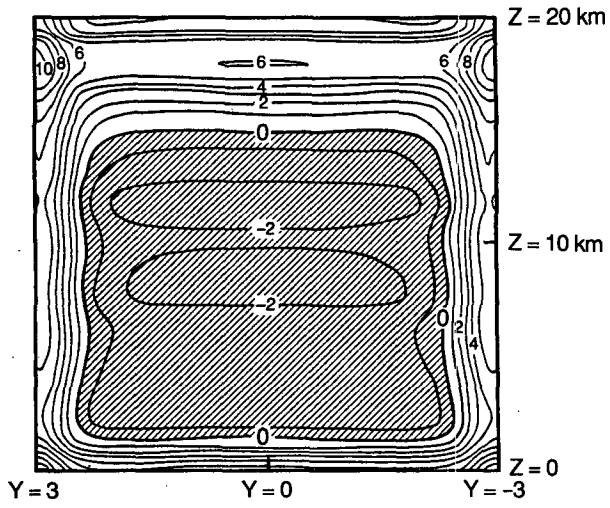

FIG. 1. The potential function $\Lambda_0(y, z)$ used by Malguzzi and Malanotte-Rizzoli (1984) to trap a weakly nonlinear dipole (see Fig. 2). Note that Λ_0 becomes strongly positive on the northern and southern flanks preventing energy propagation out of the shaded region. Contour interval 10^{-12} m^{-2}.

alent barotropic eigenfunction (no nodes in the vertical) with a dipole structure in the north–south direction. Figure 2 shows an example of one such solitary wave taken from MR85. Note however that the domain should be stretched in the x direction to give a true indication of the long-wave scaling and also that the wave as shown is more intense than is strictly permitted by the weakly nonlinear approximation.

To complete our review of weakly nonlinear local structures the conditions required for the anomaly to deepen the potential well in the y and p directions are now considered. For weak perturbations the potential Λ_0 associated with the zonal flow dominates, but if the perturbation is allowed to grow to large amplitude, as in Fig. 2, then the anomaly itself will modify the trapping potential. We wish to enquire whether this modified potential is deeper or shallower, i.e., whether the growth to finite amplitude stabilizes or destabilizes the anomaly. Assuming that the functional form $\Lambda(\psi)$ remains the same (since the anomaly is weak and localized and the streamlines are open) we can expand in a Taylor series about $\Lambda(\psi_0)$ thus:

$$\Lambda(\psi_0 + \psi_1) \approx \Lambda_0(\psi_0) + \frac{d\Lambda}{d\psi}(\psi_0)\,\psi_1 + \cdots.$$

To determine the sign of

$$\frac{d\Lambda}{d\psi}(\psi_0)$$

consider the variations of Λ with ψ in the region of minimum $\Lambda_0(\psi_0)$. All neighboring regions have larger values of Λ_0, i.e., $d\Lambda$ is always positive. Therefore, if ψ_1 is to deepen the well we require:

$$\psi_1 > 0, \quad \text{if} \quad d\psi < 0$$
$$\psi_1 < 0, \quad \text{if} \quad d\psi > 0$$

where $d\psi$ is the change in ψ_0 corresponding to the change $d\Lambda$ in the region of the potential well. Thus the perturbation must be in a sense to make ψ more uniform in the neighborhood of the Λ_0 minimum. The same argument will apply to the perturbation potential vorticity since $\Lambda = \Lambda(q)$ and thus a deeper well is produced by a more uniform q.

The analysis presented above is only valid for weak anomalies but if one considers the weakly nonlinear dipole of MR84 (Fig. 2), it is clear that a north–south dipole in a westerly flow will satisfy the conditions for deepening the potential well. MR84 noted that the dipoles tend to enhance the local stability of the flow; the interpretation given here, in terms of a deepening of the potential well, makes clear the importance of this aspect of the weakly nonlinear solution in permitting a continuous transition to a stable finite amplitude structure.

An additional point should be mentioned here for completeness. Weakly nonlinear waves are often constructed in narrow channels with confining meridional walls (e.g., Redekopp 1977). In this case the anomaly may be confined more by the lateral boundary conditions than by the structure of the zonal flow within the channel. The boundaries can be thought of as infinite potential barriers which prevent the anomaly from existing outside of the channel. Similar considerations apply when an upper rigid lid boundary condition is imposed.

To summarize then, a weakly nonlinear solitary wave is confined in all directions by the existence of a potential well. In the meridional and vertical the well is deep and is determined by the mean zonal flow potential $\Lambda_0(y, p)$. In the zonal direction the potential varies only weakly as a consequence of the presence of the solitary wave itself. However, if the wave is to re-

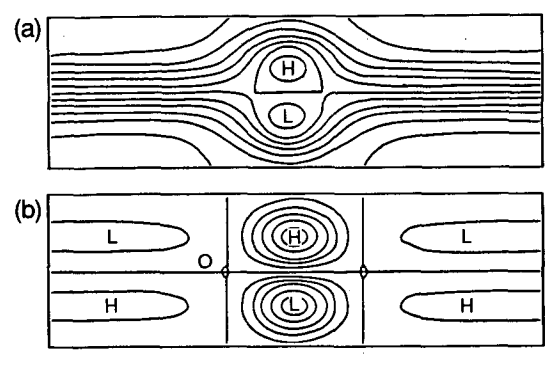

FIG. 2. (a) Total streamfunction, and (b) anomaly pattern at 500 mb for the analytic solitary wave of Malguzzi and Malanotte-Rizzoli (1985). The domain is 6000 km wide by 30 000 km long. The aspect ratio of the figure does not therefore reflect the extended longitudinal scale of the dipole required by weakly nonlinear theory. Contour interval 100 m.

main stable as it grows to large amplitude, as has been observed to occur in numerical simulations, (e.g., Boyd 1985; Haines 1987a), then it should have a form consistent with deepening the local potential well. A blocked flow with a north–south dipole structure in a westerly shear flow has the required form and is thus likely to be an inherently stable structure.

b. Strongly nonlinear modons

Modons are isolated vortex pairs existing in a uniform zonal flow (see Fig. 3) which satisfy the exact equation for steady inviscid quasi-geostrophic flow, Eq. (1); see, for example, Flierl et al. (1980), McWilliams (1980) or HM. They are constructed by allowing the functional relationship between q and ψ, and hence $\Lambda \equiv dq/d\psi$ to change discontinuously on moving from open to closed q contours. The potential Λ is more negative inside a circle of radius r_0 than outside, thus providing a "resonant cavity." To illustrate the relationships with the weakly nonlinear theory presented above, the requirements for the analytic construction of modons in a stratified fluid are reviewed.

Beginning with Eq. (1) it is assumed that the potential function associated with the zonal flow is a function of pressure alone, i.e., $\Lambda_0 = \Lambda_0(p)$. Thus, unlike the weakly nonlinear approach, there is no possibility of the far field flow confining the solution meridionally, although vertical trapping is still possible. Separable solutions of the form

$$\psi_1 = \Psi(x, y)\phi(p)$$

are sought leading to the following eigenvalue problem for the vertical structure

$$f_0^2 \frac{d}{dp}\left(\frac{1}{\sigma_{\text{ref}}}\frac{d\phi}{dp}\right) + (\lambda - \Lambda_0)\phi = 0 \qquad (10a)$$

with boundary conditions

$$\frac{1}{\phi}\frac{d\phi}{dp} = \frac{1}{U_0}\frac{dU_0}{dp} \quad \text{at} \quad p = p_s$$

$$\phi \to 0 \quad \text{as} \quad p \to 0$$

and for the horizontal structure of the wave

$$\nabla^2\Psi = \lambda\Psi \qquad (10b)$$

with boundary conditions $\Psi \to 0$ as $x, y \to \infty$ for isolation. Equation (10b) is just the two-dimensional form of Eq. (7b) but now, because of the assumed linearity between q and ψ, it is not necessary to neglect any nonlinear terms. Therefore any perturbation satisfying Eq. (10b) will also satisfy $J(\psi_1, q_1) = 0$ and so will be a solution to the fully nonlinear problem.

In order to obtain a horizontally confined solution, Λ_0, and hence λ, must be positive on open contours ensuring that ψ_1 decays away to zero in the far field. This is the "modon existence condition" discussed, for example, in HM. If λ is negative then the far field solution is oscillatory and takes the form of stationary Rossby waves. The eigenvalues of Eq. (10a) will form an ordered set with the lowest eigenvalue λ_0 corresponding to an equivalent barotropic vertical structure and λ_1 corresponding to the first baroclinic mode etc., where

$$\lambda_0 < \lambda_1 < \lambda_2 \ldots .$$

Therefore if λ_0 is positive it follows that all of the solutions have λ positive and no stationary Rossby waves are possible at all. This then provides a general condition for the existence of isolated solutions in flows for which $\Lambda_0 = \Lambda_0(p)$.

However, a problem immediately arises in the meteorological context in which the zonal flow $U_0(p)$ is westerly. In this case:

$$\Lambda_0(p) = -\frac{1}{U_0}\left[\beta - f_0^2 \frac{d}{dp}\left(\frac{1}{\sigma_{\text{ref}}}\frac{dU_0}{dp}\right)\right]. \qquad (11)$$

Substituting into Eq. (10a), multiplying by U_0, integrating vertically and applying boundary conditions it is straightforward to show that:

$$\lambda = -\beta \frac{\int \phi dp}{\int U_0 \phi dp}.$$

Thus with U_0 positive the lowest eigenvalue, corresponding to the pseudobarotropic mode ϕ_0 (with no nodes in the vertical), must be negative and so cannot represent an isolated structure. To circumvent this, in the equivalent barotropic modon studies, the form of Λ_0 is fixed independently of U_0 so as to ensure that λ is positive in the far field. This could be thought of as modifying the effective β in Eq. (11). Then if Eq. (10a) is projected onto the equivalent barotropic mode we obtain:

$$(-\hat{k}_\rho^2 + \lambda_0 - \hat{\Lambda}_0)\phi_0 = 0$$

and so

$$\lambda_0 = \hat{\Lambda}_0 + \hat{k}_\rho^2 \qquad (12)$$

where $\hat{\Lambda}_0$ is the projection coefficient of Λ_0 onto ϕ_0 and $-\hat{k}_\rho^2$ is the projection coefficient of

$$f_0^2 \frac{d}{dp}\left(\frac{1}{\sigma_{\text{ref}}}\frac{d\phi_0}{dp}\right)$$

onto ϕ_0. In fact $\hat{k}_\rho$ is the inverse of the Rossby deformation radius for this mode. Using Eq. (12) the condition $\lambda_0 > 0$ then becomes identical to the "modon existence condition" as expressed in Eq. (12) of HM. Inside the region $r < r_0$ the value of $\hat{\Lambda}_0$ changes implying a change in the vertical structure of the basic state flow. However the vertical structure of the anomaly, ϕ_0, is taken to be the same in the interior so that the anomalies can be matched at $r = r_0$. It is found that

$\hat{\Lambda}_0$ in the interior region must be more negative than $\hat{\Lambda}_0$ in the exterior region implying the existence of a potential well. Further details can be found in, for example, HM.

It was noted that for weakly nonlinear structures the existence of a trapping potential in the mean zonal flow is crucial to the maintenance of the local anomaly. However, if the anomaly becomes strong enough it will modify the Λ of its environment and begin to define its own local trapping potential in the meridional as well as the zonal direction. This effect becomes dominant when the streamlines and q contours close off in the anomaly region such as at the radius r_0 in modon solutions. Once this has occurred, local sources and sinks of potential vorticity can change the local value of Λ as described in Pierrehumbert and Malguzzi (1984) or HM. The eddy is then truly coherent and isolated from the far field. This interpretation is consistent with the envisaged role of coherent eddies in geophysical fluids. Such structures are thought to be regions of persistence and enhanced predictability embedded in more turbulent and unpredictable flows (Leith 1983).

To conclude then, the role of a potential function in determining the structure of local coherent eddies has been highlighted. It has been argued that for true coherence an anomaly should be strong enough to possess a region of closed streamlines and potential vorticity contours, thus trapping fluid parcels. The potential function will then exhibit a minimum within the closed contour region which is the most pertinent and identifiable dynamical signature of the coherent structure, the prototype for which is the modon shown in Fig. 3. It might be anticipated that in the blocking context nonlinearities may only be sufficiently strong to close off the q contours at *upper* levels. Lower down where they remain open, the weakly nonlinear theory might be a more appropriate description.

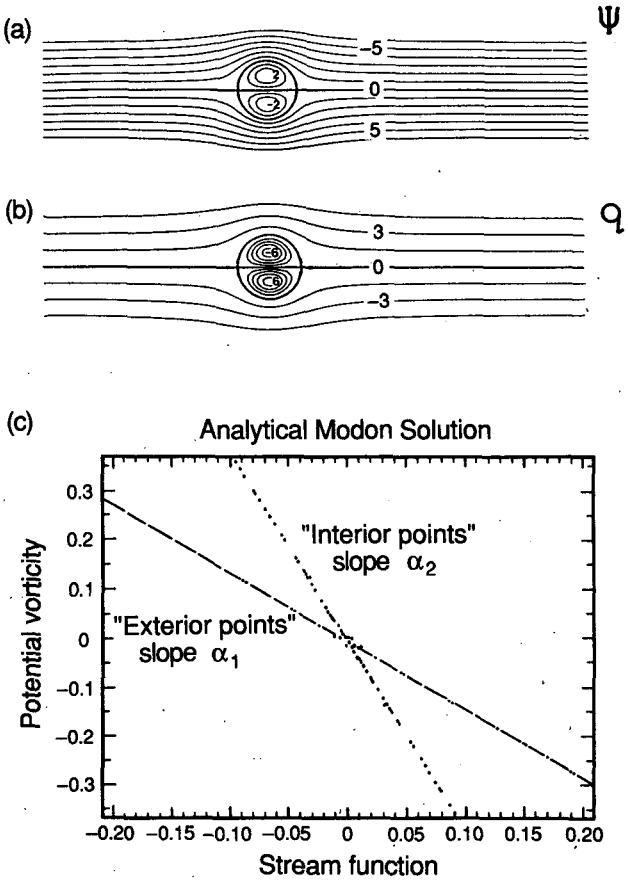

FIG. 3. (a) Streamfunction, and (b) potential vorticity for an equivalent barotropic modon in a westerly flow. (c) The scatter diagram of q against ψ, indicating that the potential $\Lambda \equiv dq/d\psi$ is more negative inside the closed contour regions than outside. Contour intervals are 10^7 m^2 s^{-1} for ψ and 1.35×10^{-5} s^{-1} for q.

3. Diagnostic study of the October 1987 block

An essential element of the theoretical models reviewed in section 2 was the existence of a suitable functional relationship between a potential vorticity, q, and a streamfunction, ψ. The discussion emphasized how the structure of the localized coherent eddies described by theory is, to a large extent, determined by the form of the potential function, $\Lambda \equiv dq/d\psi$. In this section these key features of the potential vorticity, streamfunction relationship are utilized in assessing the relevance of the modon and weakly nonlinear theories to blocking observed in the atmosphere over northeastern Europe in October 1987.

a. Data source and diagnostic framework

All the diagnostic quantities presented in this section were calculated from the global initialized analyses produced by the European Centre for Medium-Range Weather Forecasts (ECMWF). Access to the data was through a joint British Meteorological Office–University of Reading project. The data are available for the 1000, 850, 700, 500, 400, 300, 250, 200, 150, 100, 70, 50, 30 and 10 mb pressure surfaces as coefficients of spherical harmonics with a triangular truncation of T106. Analysis intervals are 6 h though for this study the diagnostics were calculated from the diurnal average of four consecutive analyses. Only the vorticity, ζ, and temperature were in fact required in calculating the derived diagnostics and both of these quantities were obtained direct from the archives without the need for further data manipulation. Where possible all calculations were performed on the spherical harmonics before transforming the results onto a 1.5 deg regular longitude–latitude grid.

In order to remain consistent with the idealized theoretical models discussed in section 2 the quasi-geostrophic form of potential vorticity was considered the most appropriate for this investigation. This was

then calculated according to the expression [see Hoskins et al. 1985, Eq. (38)]

$$q = \zeta + f + f_0 \frac{\partial}{\partial p}\left(\frac{\theta'}{d\theta_{\text{ref}}/dp}\right) \tag{13}$$

where f_0 is a constant standard value of the Coriolis parameter f, $\theta_{\text{ref}}(p)$ is a reference potential temperature distribution, and θ' the deviation from it. Here the value f_0 was chosen to be that which f would have at 60°N and the reference potential temperature was calculated, each day, as the area mean potential temperature north of 30°N. With this definition of q an appropriate streamfunction, ψ, is that representing the nondivergent component of the flow on an isobaric surface. This was obtained from ζ by action of the inverse horizontal Laplacian, a straightforward procedure with data in spherical harmonic form. Provided the quasi-geostrophic approximation remains valid the evolution of q is then governed by the equation

$$\frac{\partial q}{\partial t} + J(\psi, q) = S \tag{14}$$

together with the appropriate boundary conditions, where S represents the sources and sinks of potential vorticity.

A useful way of analyzing the relationship between q and ψ is to construct a scatter diagram by plotting the value of q against the value of ψ for each data point in the region of interest. Then if the flow pattern is of the so-called free-mode form with q functionally related to ψ the points on the diagram will lie precisely on some curve $q = q(\psi)$. On the other hand, a spread of points about $q = q(\psi)$ is an indication, at least qualitatively, of the extent to which the flow deviates from free-mode form. Apart from possible data errors this spread is a consequence of any residual time dependence in Eq. (14) and/or net sources and sinks of potential vorticity, provided that it is also assumed that all the terms neglected under the quasi-geostrophic scaling are absorbed into the source term S. In the case of time-averaged flows S would also include the forcing by the transient eddies.

Although this study is only intended to be a qualitative investigation of the relationship between q and ψ during a blocking episode, it is worth noting that with suitable choices of data points the scatter diagrams may be exploited to provide *quantitative* information about the flow. In particular Read et al. (1986) have shown that if the data points are chosen along a curve in physical space such that the corresponding curve in (q, ψ) space encloses an area α, then this area is equal to the net flux of q (by the nondivergent flow) across the curve in physical space. (In deriving this result some care is required in assigning the correct sign to α when α is made up of more than one closed curve in (q, ψ) space—see Read et al. 1986 for more details.) Furthermore, Read et al. (1986) use this result to propose the quantity

$$I = \frac{\alpha}{\Delta\psi\Delta q} = \frac{\text{area enclosed on } (q, \psi) \text{ diagram}}{\text{area of the circumscribing rectangle}} \tag{15}$$

as a measure of the extent of departure from free-mode form. In (15) the circumscribing rectangle refers to the minimum area rectangle with sides parallel to the axes and dimensions $\Delta q \times \Delta\psi$ which encloses all the points on the (q, ψ) diagram. Alternatively, Haines (1987a; see also Marshall and Nurser 1986) shows that I is also related (at the resolution of the data) to the area mean of the angle, γ, between the q and ψ contours, provided that attention is restricted to regions of physical space in which γ does not change sign. From a theoretical perspective a small value of the mean angle, $\bar{\gamma}$, is often a useful expansion parameter for expressing departures from free-mode form (HM; Pierrehumbert and Malguzzi 1984). However, because of the difficulties involved in assigning the correct sign to α or in identifying regions of physical space in which γ does not change sign, extracting quantitative information from the scatter diagrams can, in practice, be rather complicated, and was not considered necessary for the present study. Nevertheless, it should be emphasized that the results of Read et al. (1986) and Haines (1987a) do provide the theoretical basis that justifies the qualitative interpretation of the scatter diagrams presented below. A more detailed series of diagnostics using these techniques may subsequently yield valuable quantitative information on the time evolution of blocks and on the role of forcing and dissipation mechanisms.

b. *Results*

Apart from the results shown in Figs. 11 and 12, all of the diagnostics presented in this section utilize five-day mean data centered on the specified date. In effect this removes most of the contribution of the transient eddies which, while generally acknowledged as being important for maintaining blocks (e.g., Shutts 1986), do *not* directly contribute to the zero order balances of the free-mode state for which the modon and weakly nonlinear theories are the proposed idealized models. Attention is focused mainly on the 300 mb level where the flow is most intense and nonlinear effects are expected to have their strongest influence. Throughout this section the units of ψ are 10^7 m^2 s^{-1} and those of q and $f + \zeta$ are 10^{-5} s^{-1}.

Figure 4 shows a sequence of the five-day running mean ψ and q fields on the 300 mb surface during the mature stage of a blocking episode observed in October 1987. The streamfunction shown in the left-hand pictures indicates that the characteristic blocking signature of a split flow was already present over central Europe on 19 October and remained at roughly the same lo-

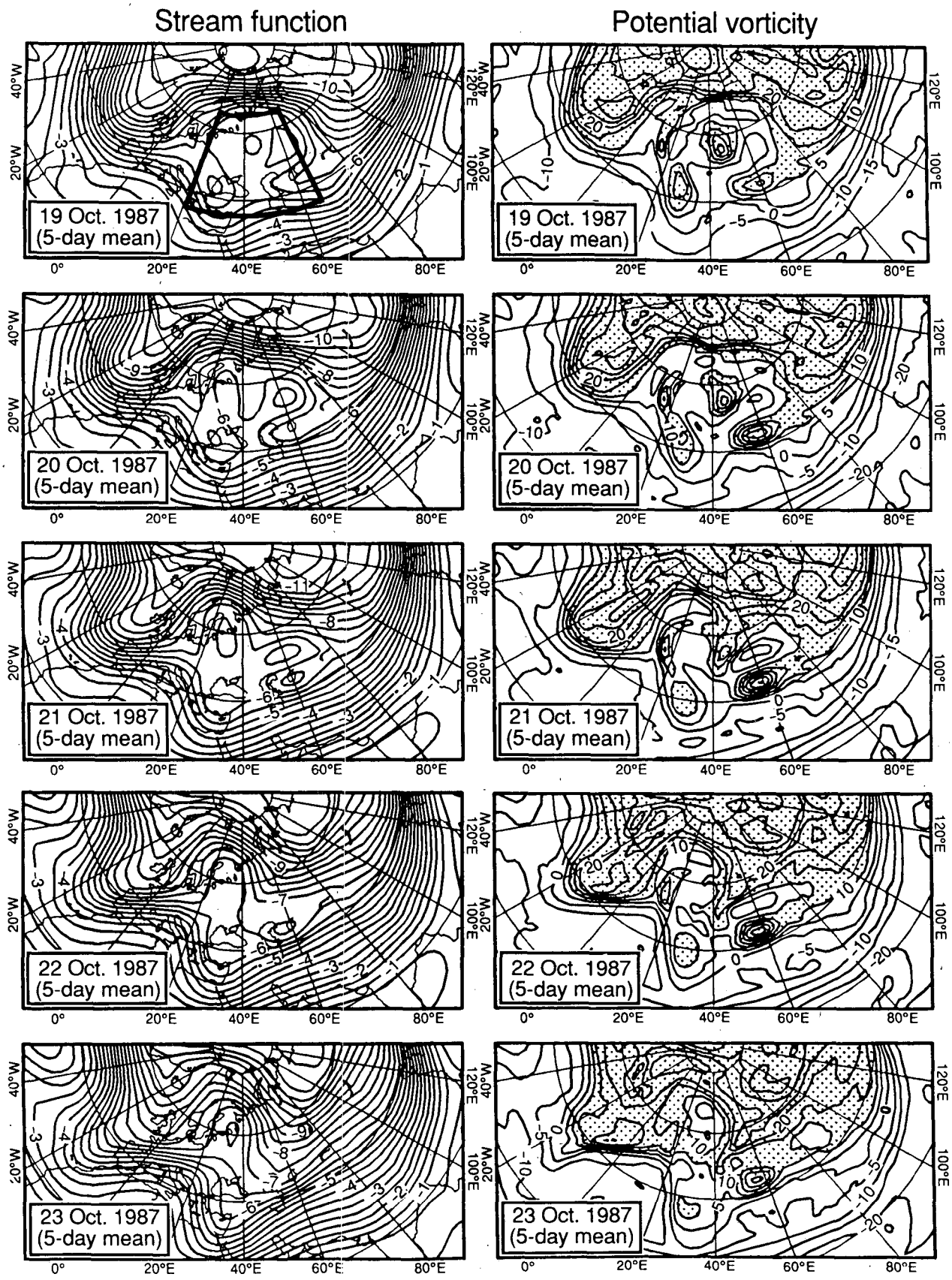
Stream function
Potential vorticity
19 Oct. 1987 (5-day mean)
20 Oct. 1987 (5-day mean)
21 Oct. 1987 (5-day mean)
22 Oct. 1987 (5-day mean)
23 Oct. 1987 (5-day mean)
0°
20°E
40°E
60°E
80°E
40°W
20°W
120°E
100°E

cation on the following four days. (The overbar over the date will be used to indicate that the quantity referred to is the five-day average for that date.) However, the streamfunction did not exhibit the simple structure of a single north–south dipole. Instead, on $\overline{19}$ October there were two troughs, one over the Balkans and another to the east of the Caspian Sea, with a separate cutoff anticyclone. As the block continued to develop, the central cyclone gradually disappeared while the anticyclone, and the trough to its south, strengthened to form a distinct north–south dipole around 60°E on $\overline{21}$ October. By this date a second cutoff anticyclone had developed to the north of the Balkan trough resulting in a separate dipole configuration at 30°E. Although weaker than the one further east, this dipole extended over a broader range of latitudes. By the $\overline{23}$ October the dipole structure at 60°E had decayed away altogether and the system to the west had become much less prominent.

As would be expected the quasi-geostrophic potential vorticity presented in the right-hand pictures of Fig. 4 provides a much sharper image of the structure of the block than the corresponding streamfunction. In particular it is noticeable how the block appears to be associated with a number of distinct cutoff q anomalies, most of which have high values of q. The only strong cutoff region of low q was formed on $\overline{21}$ October when the high q anomaly originally at 40°E drifted slightly eastward and linked the high q to the north to the tongue of high values further south. This cutoff region of low q had also disappeared altogether on $\overline{23}$ October. Despite this rather complex synoptic behavior, all of the features described above are from the 5-day mean fields and are therefore persistent on this time-scale.

The scatter diagrams corresponding to the q and ψ fields shown in Fig. 4 are presented in Fig. 5. The diagrams were constructed from data on the 1.5-degree longitude–latitude grid but using only those values from grid points in the latitude band 36° to 66°N and in the quadrant 50°W to 130°E. Crosses are used to highlight data from the subquadrant 21° to 66°E (bounded by the thicker grid lines in the upper left-hand picture of Fig. 4) where the block was almost entirely situated. The dots, therefore, represent data points from outside the block and these congregate fairly closely about roughly the same straight line in all five diagrams. The straight line indicates an approximately linear functional relationship between q and ψ such that outside the block the potential Λ ($\equiv dq/d\psi$) is very nearly horizontally constant. This is consistent with the earlier results of, for instance, Illari and Marshall (1983) and Derome (1984) but the underlying reasons why many observed flow patterns appear to favor a linear functional relationship are not well understood, a point which is returned to in section 4.

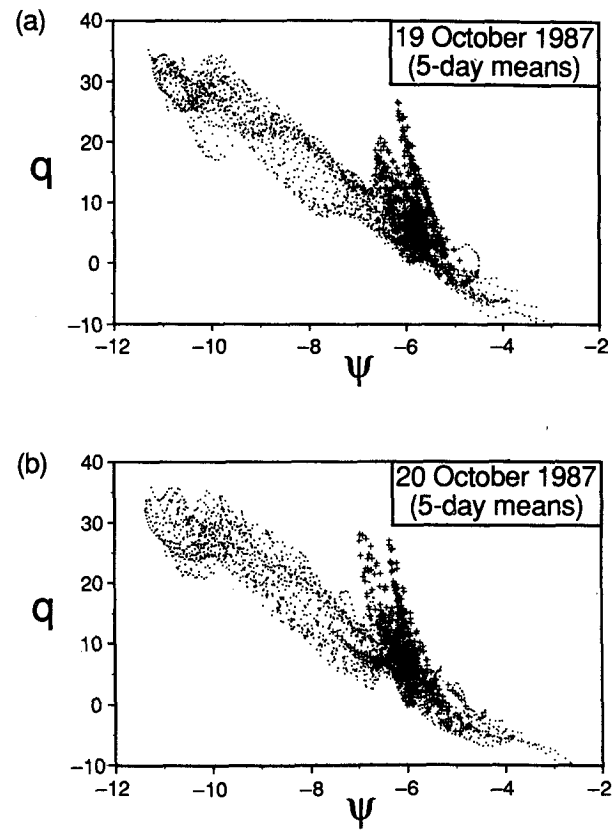

FIG. 5. (a) Scatter diagram of the five-day mean grid point values of streamfunction ψ, and quasi-geostrophic potential vorticity, q, at 300 mb, for the 19 October 1987. Dots, (·) indicate values for data points in the latitude band 36° to 66°N and in the quadrant 50°W to 130°E. Values from data points in the region extending from 21° to 66°E and bounded by the thicker grid lines in the upper left hand map of Fig. 4 are indicated with crosses, (+). Units of ψ are 10^7 m^2 s^{-1}, and those of q are 10^{-5} s^{-1}. (b) As Fig. 5a but the five-day mean values for the 20 October 1987.

The crosses in Figs. 5a–d clearly indicate the different character of the relationship between q and ψ in the vicinity of the block. There is evidence of two approximately linear functional relationships from $\overline{19}$ to $\overline{22}$ October inclusive. In fact, a more detailed analysis of

FIG. 4. Streamfunction, ψ (left-hand maps), and quasi-geostrophic potential vorticity, q (right-hand maps), at 300 mb. The fields shown are 5-day means centered on the date indicated on the individual maps. Contour intervals are 0.5×10^7 m^2 s^{-1} for ψ and 5×10^{-5} s^{-1} for q. In the right-hand maps, areas where q has a value greater than 10×10^{-5} s^{-1} are shaded. The vertical longitude is 40°E and the latitude circles are 20°, 40°, 60° and 80°N. The "blocking region" is indicated in the upper left-hand map by the thicker grid lines at 36° and 66°N, and at 21° and 66°E. In all the subsequent scatter diagrams (Figs. 5, 8, 10 and 12) crosses (+) will be used to indicate values from within this region and dots (·) will indicate the values from the remaining part of the latitude band between 36° and 66°N which appears on the maps.

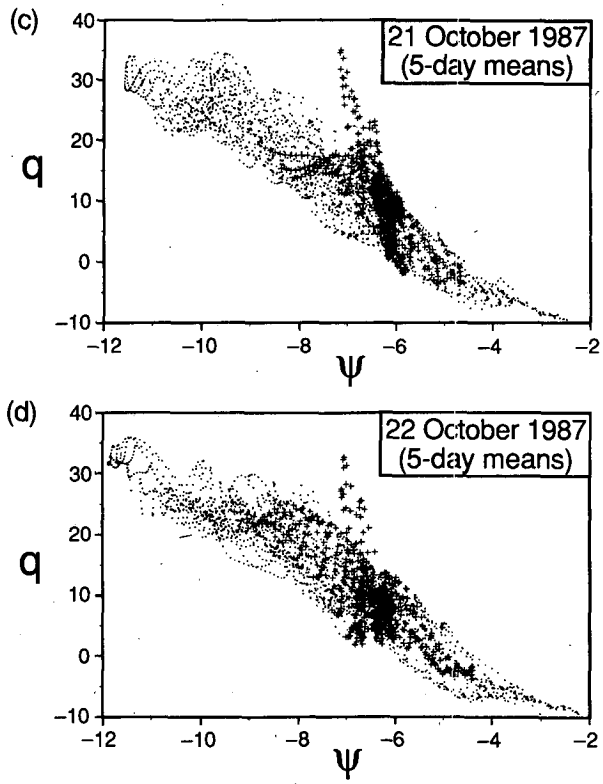

FIG. 5. (c) As Fig. 5a but the five-day mean values for the 21 October 1987. (d) As Fig. 5a but the five-day mean values for the 22 October 1987.

the data suggests that points from each individual region of closed q contours in Fig. 4 are likely to be spread about different lines in (q, ψ) space. In every case, however, the lines in (q, ψ) space representing these local anomalies have a more-negative slope than the line associated with points from outside the blocking region. The general absence of crosses from below, and to the left, of the cluster of dots in Figs. 5a–d probably reflects the bias towards cutoff areas of high q present in Fig. 4. Otherwise, the signature seen in Figs. 5a–d is very reminiscent of that of the isolated modon structures in theoretical models (cf. Fig. 3). In particular there is clear evidence in Fig. 5 that within the cutoff q anomalies there was a deepening of the potential well associated with a localized minimum of the potential function $\Lambda \equiv dq/d\psi$. Outside the block the potential was fairly constant and remained unchanged as the block developed and eventually began to decay. This perhaps constrasts with the observations of Malanotte-Rizzoli and Hancock (1987) who appear to detect a trapping potential upstream of a composite blocking flow. Here, the form of the potential function is more consistent with that required in the modon model than in the weakly nonlinear theories and supports the view that the self-trapping mechanism of a modon (see section 2) played an important role in sustaining the observed local structures. By $\overline{23}$ October, however, the crosses were almost entirely within the spread of dots (Fig. 5e) indicating that there was no longer a well-defined confining localized minimum in Λ which is consistent with the decay of the block seen in Fig. 4. Again, it is worth noting that there is no obvious evidence from the scatter diagrams of a change in the form of Λ outside the blocking region on this day.

The variation of q with ψ across the blocking region on $\overline{21}$ October is shown in Figs. 6a and 6b for the latitudes 45° and 54°N, respectively. In these diagrams the value of q has been plotted against the value of ψ (again, 5-day means) for each grid point between 50°W and 130°E at the designated latitude and the points joined up in order of longitudinal position. Points on the resultant curves corresponding to the grid points at 21° and 66°E are marked by the solid rectangles while the dots are used to indicate the values from the intermediate grid points.

Immediately apparent from the two diagrams is the obvious zonal dependence of q and ψ both inside and outside the blocking region. Also apparent is the abrupt change in the form of the curves which occurs on entering and leaving the location of the block. Upstream of the block both curves form single narrow loops whose enclosed areas are, according to the results of Read et al. (1986), equal to the meridional fluxes of q (by the time-averaged rotational flow) in the corresponding zonal ranges at the respective latitudes. The relatively small size of these areas suggests that the fluxes are rather small, particularly at 54°N. As the latitude circles enter the region of the block, somewhere just west of 21°E, the curves in Figs. 6a and 6b adopt a much steeper orientation. In Fig. 6b that segment of the curve constructed from values of q and ψ within the block is dominated by two sharp peaks, slightly displaced from one another, indicating the presence of the two separate cutoff q anomalies seen in Fig. 4. In this case the left hand peak is the result of the high q anomaly seen at about 18°E on $\overline{21}$ October in Fig. 4 and the right hand peak is caused by the presence of

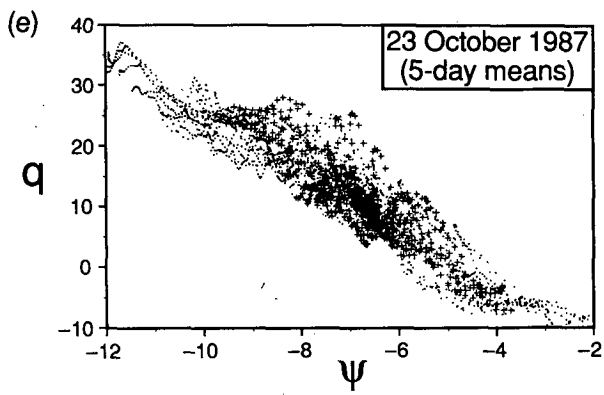

FIG. 5e. As Fig. 5a but the 5-day mean values for the 23 October 1987.

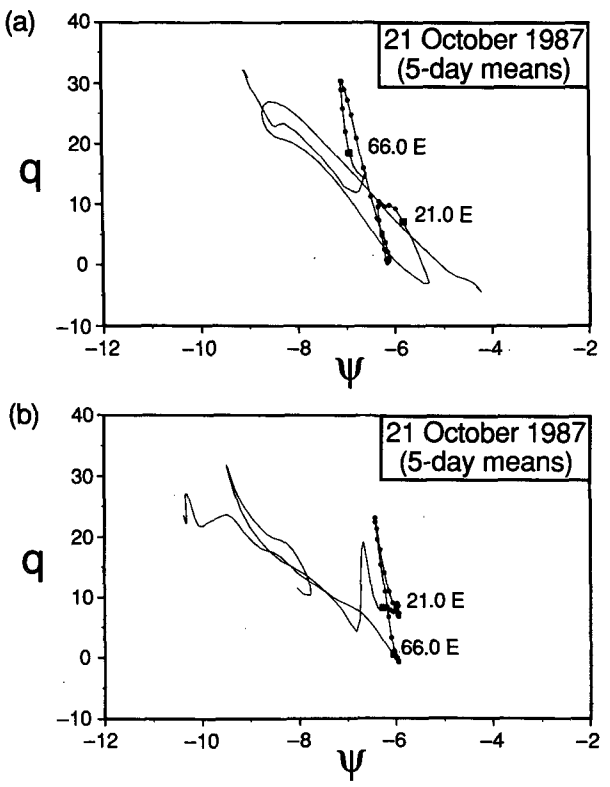

FIG. 6. (a) Five-day mean values of potential vorticity, q, and streamfunction, ψ, at 300 mb for the 21 October 1987. The value of q is plotted against the value of ψ for each grid point between 50°W and 130°E along the latitude circle at 45°N and the points joined up in order of longitudinal position. The solid rectangles indicate the (q, ψ) values from the grid points at 21° and 66°E and dots indicate the values from the intermediate grid points. Units of q and ψ are the same as in Fig. 5a. (b) As Fig. 6a but for latitude 54°N.

the relatively high q values between 40° and 45°E for the same period. Figures 6a and 6b also show the contrast between the high and low components of the north–south dipole seen at 60°E on $\overline{21}$ October in Fig. 4. The low q at 54°N is associated with a cluster of dots on the curve in Fig. 6b indicating the rather flat nature of the anticyclone, i.e., weak q gradients. On the other hand, there is a spacing out of those dots in Fig. 6a which denote the q, ψ values within the cyclone at 45°N and the high q anomaly appears in this figure as a distinct peak. Downstream of the block the curves in both diagrams are roughly parallel to the major axes of the upstream loops. This suggests that, insofar as the flow is of approximate free-mode form, the linear functional relationship between q and ψ is the same upstream as downstream of the block.

A possible cause for concern with the results presented so far is the application of the quasi-geostrophic approximation in the vicinity of the tropopause. In particular, calculating q using a reference potential temperature distribution, $\theta_{\text{ref}}(p)$, based on an area average over a large domain, may not be entirely appropriate for isobaric surfaces that intersect the tropopause. For these surfaces it is unlikely that the large differences in static stability between the stratospheric and tropospheric regions will be correctly captured when using an *area mean* reference potential temperature distribution and, without further information, it is conceivable that some of the features identified as being important in Figs. 5 and 6 may be spurious. In order to examine this possibility the preceding analysis was repeated using absolute vorticity, ζ_a ($\equiv f + \zeta$), instead of q. Only the results for $\overline{21}$ October are shown but similar conclusions were obtained when considering the other 4 days.

Figure 7 shows the five-day mean absolute vorticity at 300 mb for $\overline{21}$ October. Comparing this figure with the potential vorticity field shown in Fig. 4 for the same day confirms that the blocking signature seen in the potential vorticity was not merely a consequence of changes in static stability across the tropopause. In fact, it turns out that the absolute vorticity and stretching term [right-hand term in Eq. (13)] contribute almost equally in determining the spatial structure of q within the vicinity of the block.

The relationship between ζ_a and the streamfunction ψ is displayed in the scatter diagram in Fig. 8. Dots and crosses in this diagram represent the same data points as in Fig. 5 but note the different scale for the ordinate. In many respects the scatter diagram of the isolated modon structures from theoretical models (cf. Fig. 3) is more like that in Fig. 8 than the (q, ψ) diagram presented in Fig. 5c. Unlike Fig. 5c the "interior branch" (which is more negatively sloping) of the $\zeta_a(\psi)$ curve identifiable in Fig. 8, extends below the "exterior branch" of the curve. This is clearly the signature of the blocking anticyclone which is seen in Fig. 4 at around 60°E. The other main difference between Figs. 5c and 8 is in the ranges of q and ζ_a. Outside the block the range of q is much greater than that of ζ_a as a result of the large differences in the stretching term between

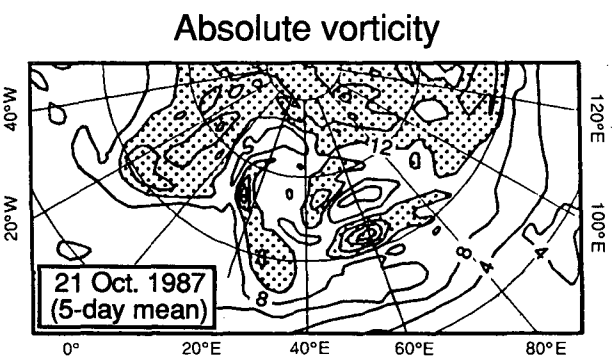

FIG. 7. Five-day mean absolute vorticity, ζ_a, at 300 mb for the 21 October 1987. The contour interval is 4×10^{-5} s^{-1} and areas where ζ_a has a value greater than 12×10^{-5} s^{-1} are shaded. The map grid is as in Fig. 4.

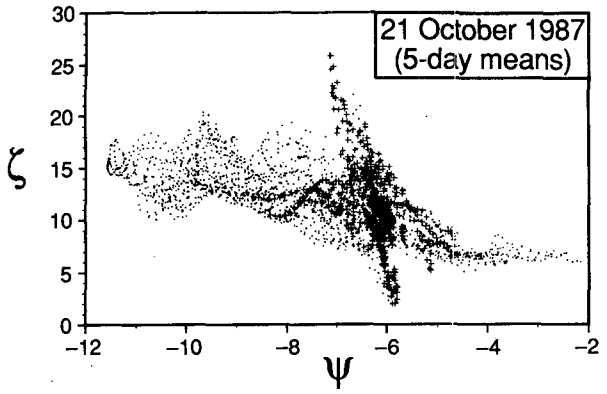

FIG. 8. Scatter diagram of the 5-day mean grid point values of streamfunction, ψ, and absolute vorticity, ζ_a, at 300 mb for the 21 October 1987. The corresponding ζ_a contour map is shown in Fig. 7. The dots (·) and crosses (+) indicate values from the same data points as in Fig. 5. Units are 10^7 m^2 s^{-1} for ψ and 10^{-5} s^{-1} for ζ_a.

the polar stratospheric air and the midlatitude tropospheric air. Within the block the ranges of q and ζ_a are roughly comparable, again registering the importance of the contribution of absolute vorticity in determining the q anomalies of the blocking configuration. Therefore, as the stretching term apparently does not dominate the blocking signatures in the 300 mb q field, or the form of the relationship between q and ψ, it is reasonable to assume that any doubts about the use of the quasi-geostrophic approximation at the 300 mb level are unlikely to affect the interpretation of the diagnostics presented here or the final conclusions.

An interesting aspect of Fig. 8 is the suggestion of an approximately linear functional relationship between ζ_a and ψ, in addition to that between q and ψ. [As both functions are linear the stretching term must also be an approximate linear function of ψ, as is confirmed by the appropriate scatter diagram (not shown).] The existence of this second functional relationship between ζ_a and ψ probably reflects the fact that the flow is not only of approximate free-mode form but is also equivalent-barotropic. Certainly, when the five-day mean 500-mb streamfunction map for $\overline{19}$ October (Fig. 9a) is compared to the 300 mb streamfunction in Fig. 4, there is clear evidence of the barotropic nature of the flow. Although not shown, similar conclusions were also obtained on comparing the 300 and 500 mb mean streamfunctions on the following four days. However, at 500 mb the five-day mean potential and absolute vorticity anomalies associated with the block on $\overline{19}$ October are very much weaker than those at 300 mb and are not so clearly identified in Figs. 9b and 9c, respectively (cf. Figs. 4 and 7 for the 300 mb fields). Nevertheless, the corresponding (q, ψ) and (ζ_a, ψ) scatter diagrams shown in Figs. 10a and 10b (again, the dots and crosses represent the same data regions as in Fig. 5) show some evidence of separate functional relationships within the region of the block, but the points on the (q, ψ) diagram from outside the blocking region are fairly well spread out. In fact, the spread of dots in Fig. 10a is such that if the crosses had not been used to highlight values from the location of the block it would not have been possible to detect the approximate functional relationship in that region. However, because of the different scales of the axes it is likely that the flux of q connected with the spread of dots in Fig. 10a is no greater than that at 300 mb (cf. Fig. 5a).

The approximate free-mode behavior found when considering the five-day mean fields implies that the relatively steady blocking pattern was accompanied by a close balance between the forcing by the high fre-

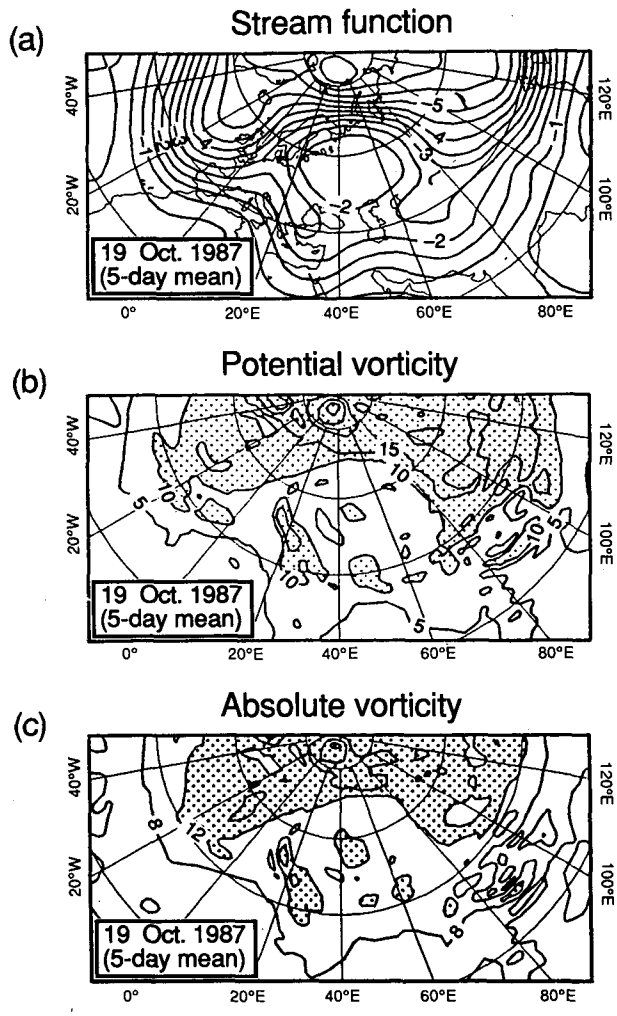

FIG. 9. (a) Five-day mean streamfunction at 500 mb for the 19 October 1987. The contour interval is 0.5×10^7 m^2 s^{-1}. (b) Five-day mean potential vorticity, q, at 500 mb for the 19 October 1987. The contour interval is 5×10^{-5} s^{-1}. Areas where q values are greater than 10×10^{-5} s^{-1} are shaded. (c) Five-day mean absolute vorticity, ζ_a, at 500 mb for the 19 October 1987. The contour interval is 4×10^{-5} s^{-1}. Areas where ζ_a values are greater than 12×10^{-5} s^{-1} are shaded.

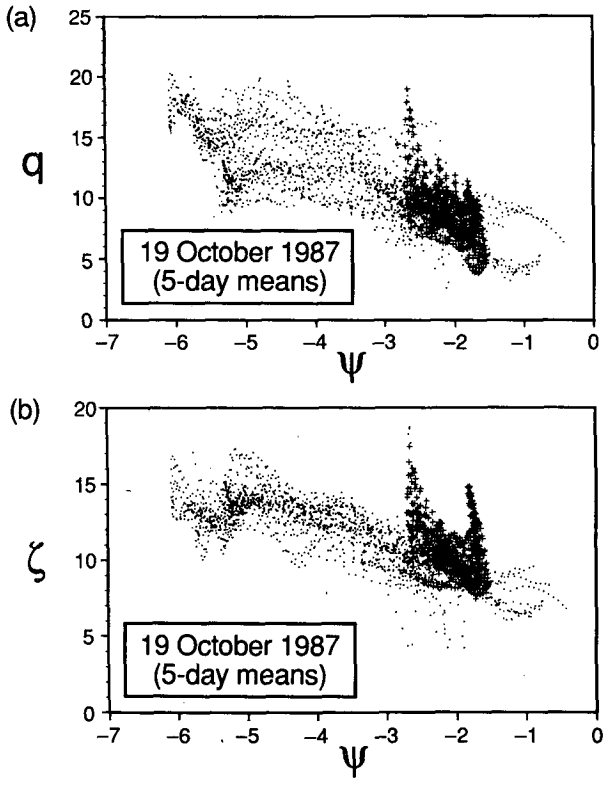

FIG. 10. (a) Scatter diagram of the 5-day mean grid point values of streamfunction, ψ, and quasi-geostrophic potential vorticity, q, at 500 mb for the 19 October 1987. Figures 9a and 9b show the corresponding contour maps. The data regions and units are as in Fig. 5. (b) Scatter diagram of the 5-day mean grid point values of streamfunction, ψ, and absolute vorticity, ζ_a, at 500 mb for the 19 October 1987. Figures 9a and 9c show the corresponding contour maps. The data regions are as in Fig. 5. Units of ζ_a and ψ are as in Fig. 8.

quency transient eddies and the dissipation. (Note that in the case of the results for absolute vorticity the balance will also include any divergence forcing of the rotational flow.) An indication of the instantaneous contribution of the transient eddies to the daily q and ψ fields at 300 mb during and after the blocking dipole episode may be obtained from Fig. 11. The upper two maps are for 21 October when the blocking was most prominent. Comparing these two maps with the 5-day mean maps for the same day (Fig. 4) indicates that the temporal averaging on this day had little effect on the overall spatial structure of the q and ψ fields, except in reducing the amplitudes of the individual features. The lower two maps in Fig. 11 show that by 25 October there was very little remaining evidence of a blocking pattern in the daily fields of q and ψ.

Scatter diagrams constructed from the daily values of q and ψ for 21 and 25 October are presented in Figs. 12a and 12b, respectively. Again the dots and crosses represent the same data regions as in Fig. 5 but the range of the q-axis has been extended. Apart from a general increase in scatter the diagram for 21 October (Fig. 12a) is remarkably similar to that shown in Fig. 5 constructed from the five-day mean values. The daily values in Fig. 12a clearly show evidence of two different, approximately linear functional relationships between q and ψ. The more negatively sloping line is associated with values of q and ψ from the block and represents a deepening of the potential well within that location (cf. section 2). The link between this more steeply sloping line and the existence of the block is further established by a comparison with the scatter diagram shown in Fig. 12b constructed from the daily values of q and ψ on 25 October. As previously stated the instantaneous maps of q and ψ for this day (lower two pictures in Fig. 11) contain very little remaining evidence of the block and likewise all the dots and crosses in Fig. 12b appear to be spread about roughly the same, single, straight line as the dots in Fig. 12a. The absence of any evidence for a second functional relationship in Fig. 12b implies that there was no longer a localized minimum of the potential function Λ on 25 October, suggesting that the minimum present on 21 October was clearly associated with the existence of the block. Moreover, the failure of the contribution from the transient eddies to mask the signal of the change in form of the potential function Λ in Fig. 12 is perhaps an indication that the type of self-trapping mechanism operating in the modon model is particularly relevant to the blocking processes observed in the atmosphere.

4. Discussion and conclusions

In this paper an attempt has been made to present a unifying theme as a basis for the investigation of solitary wave models of blocking. The potential function $\Lambda \equiv dq/d\psi$ was identified from theoretical considerations in section 2 and it was shown that many of the well-known properties of solitary waves can be understood as consequences of the spatial variations of this quantity. In section 3 the powerful scatter diagram diagnostic was used to determine the spatial and temporal variations of Λ during a particular blocking episode in October 1987.

Several important questions are raised by our theoretical and observational treatment which deserve further discussion. The theoretical development in section 2 assumes the quasi-geostrophic framework and therefore this framework was also used for analyzing the data. Inevitably this means that the diagnostics require some care in their interpretation. Unfortunately, there is as yet no theory which adequately describes isolated, coherent structures in the primitive equation framework. Indeed, an analog of the "potential function" may be difficult to find in more general equation systems as the definition requires an unambiguous separation of the "basic state flow" and the "perturbations." Nevertheless, functional relationships between the Ertel potential vorticity and an appropriate streamfunction

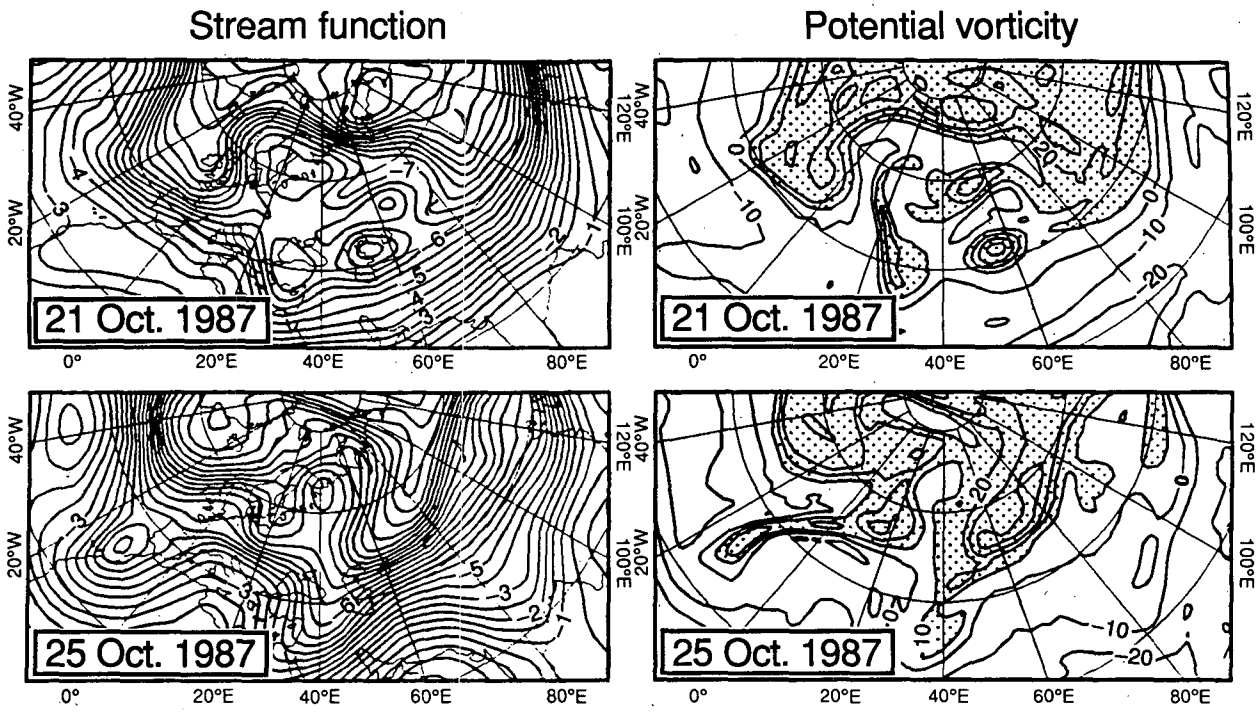

FIG. 11. The daily streamfunction, ψ, (left-hand maps) and potential vorticity, q, (right-hand maps) on the 21 and 25 October 1987. Contour intervals are 0.5×10^7 m^2 s^{-1} for ψ and 10×10^{-5} s^{-1} for q. The map grid lines are the same as in Fig. 4.

can still provide useful information for analyzing and diagnosing free-mode flows in the framework of the full primitive equations (White 1985, personal communication). Strictly speaking, however, the interpretation of the functional relationships found in the data in terms of trapping potentials must be made within the quasi-geostrophic framework and can be considered only to be relevant to the extent to which the atmosphere can be considered a quasi-geostrophic system.

Some of the results presented in section 3 appear to exhibit significant discrepancies with the idealized dipole blocking models of section 2. It is clear from Fig. 4 that this blocking episode cannot be entirely represented by a north–south dipole anomaly in the potential vorticity field. Instead, there appear to be several isolated cyclonic vortices coexisting within the blocking region. In contrast, there is only one well-formed coherent anticyclone present, although the low q anomaly does remain aligned to the north of one of these cyclonic anomalies at around 60°E producing a persistent dipole. The asymmetry between the cyclonic and anticyclonic q anomalies is also evident in the scatter diagrams in Fig. 5 where it was noted that there was no apparent signature of a low q anomaly in the blocking region. The preponderance of high q anomalies is probably related to the bias towards intense cyclonic anomalies caused by gradient wind effects. Low q anomalies are necessarily less intense with weaker q gradients and are therefore less coherent. It is possible that the signature of the coherent anticyclone which is seen in Fig. 4 may be masked in Fig. 5 by an inappropriate definition of vortex stretching close to the tropopause, another difficulty inherent in the quasi-geostrophic analysis. Nevertheless, in the scatter diagram constructed for a single latitude, Fig. 6b, there is some evidence of the low q anomaly contributing to the steeper "interior" branch of the functional curve. Furthermore, when the absolute vorticity scatter diagram is plotted in Fig. 8 the evidence for the anomalous anticyclone is unmistakable.

Despite these problems, the evidence presented for the existence of a local minimum in the potential Λ seems to be conclusive and this observation, which has a clear interpretation within the theoretical framework of solitary waves, implies that local nonlinear dynamics play an important role in determining the structure and persistence of blocking events. The results are entirely consistent with the view of blocking propounded by Illari (1984), Hoskins et al. (1985), and Shutts (1986), except that here, emphasis is placed on the inherent stability of coherent dipoles as an important factor in determining the longevity of many blocking events. On the other hand, our observations are inconsistent with theories which attempt to represent blocking as a superposition of global stationary Rossby waves: such a superposition of waves would not present any anomalous signature at all on a (q, ψ) scatter diagram. Unlike Malanotte-Rizzoli and Hancock (1987), no evidence was found in the data for the potential Λ becoming positive anywhere as strictly required by

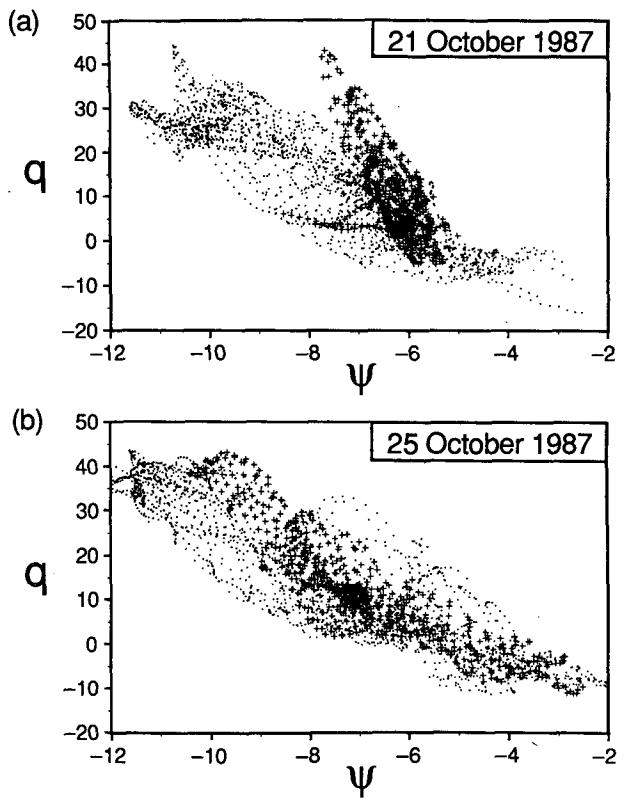

FIG. 12. (a) Scatter diagram of the daily values of streamfunction, ψ, and potential vorticity, q, on the 21 October 1987. The corresponding contour maps are shown in Fig. 11. The dots (·) and crosses (+) indicate values from the same data points as in Fig. 5. The units of q and ψ are also the same as in Fig. 5. (b) As in Fig. 12a but for the (q, ψ) values on the 25 October 1987.

weakly nonlinear theory (see section 2). However, it is suggested that the presence of a deep potential well can still lead to the trapping of a local structure despite the leaking of energy in the form of Rossby wave radiation which, along with diabatic processes and Ekman friction acting at the surface, may contribute to the decay of the block. Modeling studies enquiring into this possibility have shown promising results.

Transient eddy interactions are now generally acknowledged to play an important role in the maintenance of blocks. In the light of the analysis presented in section 2 it is clear that the interaction with synoptic eddies will be enhanced if the block is associated with a minimum in Λ. An increase in the local refractive index (i.e., a deepening of the potential well) will tend to focus eddy activity, leading to deposition of eddy energy which can reinforce the blocking flow. This effect was noted in Hoskins et al. (1983) who comment on the tendency of E-vectors to point inwards towards the center of blocking regions. This focusing can also be seen in the E-vector diagnostics in the barotropic numerical study of HM (see their Fig. 10). Thus it seems that both the inherent stability of blocking configurations and their excitation by synoptic scale systems will be enhanced if the winds are configured in such a way as to create a local resonant cavity or potential well. However, despite the attractiveness of this interpretation there are many questions that remain unanswered. In particular, processes which control the initial formation of blocks have not been considered.

It was suggested by Malanotte-Rizzoli and Hancock (1987) that blocking might be preceded by a deepening of the potential well associated with the zonal flow, thus preconditioning the flow towards trapping in the meridional and vertical directions. Their diagnostics, however, show no sign of such a preconditioning. Our results are consistent in revealing a potential well signature only when the block is fully mature with cutoff vortices present within the blocked region. Nevertheless, it may be worth pursuing this idea with more detailed studies since the rewards for identifying a preblocking flow would be very great.

The interpretation presented here suggests that the potential well will be formed as the streamlines and potential vorticity contours close off. Several studies throw some light upon the possible mechanisms by which this process may occur. Pierrehumbert and Malguzzi (1984) suggest that weak forcing and dissipation processes acting within closed time-mean contours can help to set the functional relationship. In attaining a suitable balance between forcing and dissipation the $q(\psi)$ relationship will adjust within the cutoff vortices of a block, thus modifying the potential Λ.

An alternative interpretation is suggested by Stern (1975) and Leith (1984), who propose that the flow within cutoff vortices will adjust to a state of local minimum enstrophy (assuming two-dimensional turbulence dominates). They show that this implies a linear functional relationship between q and ψ within the vortices and that the constant of proportionality (i.e., the potential) may be different from the exterior potential, thus allowing the development of a trapping minimum.

Recent work by Couder and Basdevant (1986) provides a further possible explanation for the linearity of the function $q(\psi)$ within dipole vortices. They observe that dipoles with a linear functional relationship within the vortices are the most strongly coupled and the most rapidly propagating with respect to the external flow. Such dipoles will very readily form and persist in the presence of a strong meridional potential vorticity gradient as in the atmosphere. This observation also appears to explain the structure of the dipoles which were resonantly excited in the experiments of HM.

Although evidence from only a single case of blocking has been presented here, an earlier study using the scatter diagram diagnostic for data on isentropic surfaces also suggested that blocking anomalies can exhibit "modonlike" dynamics. This data for the Atlantic

blocking episode in February 1983 is presented in Haines (1987a,b). Perhaps an obvious follow-up study could examine other blocking events, including Pacific blocking using scatter diagrams to see if there is any evidence of potential well trapping. The present evidence suggests that Pacific blocks (which usually consist of just a single anticyclone rather than a dipole) could not be well-represented by the simplest β-plane modons such as that in Fig. 3. However, if observations suggest that potential well trapping is important in Pacific blocking, perhaps the asymmetric modons, which have been constructed by Verkley on a sphere, or else modons modified by external shear flow may provide more appropriate coherent eddy solutions.

Acknowledgments. The authors would like to thank Dr. A. A. White of the U.K. Meteorological Office for his useful comments and advice throughout the course of this work and the staff of the European Centre for Medium Range Weather Forecasts for their help in processing the data. Dr. K. Haines was supported by the Natural Environmental Research Council of Great Britain.

REFERENCES

Boyd, J. P., 1985: Equatorial solitary waves. Part III: Westward traveling modons. *J. Phys. Oceanogr.*, **15**, 46–54.

Butchart, N., S. A. Clough, T. N. Palmer and P. J. Trevelyan, 1982: Simulations of an observed stratospheric warming with quasi-geostrophic refractive index as a model diagnostic. *Quart. J. Roy. Meteor. Soc.*, **108**, 475–502.

Couder, Y., and C. Basdevant, 1986: Experimental and numerical study of vortex couples in two-dimensional flows. *J. Fluid Mech.*, **173**, 225–251.

Derome, J., 1984: On quasi-geostrophic, finite-amplitude disturbances forced by topography and diabatic heating. *Tellus*, **36A**, 313–319.

Flierl, G. R., 1987: Isolated eddy models in geophysics. *Annual Review of Fluid Mechanics*, Vol. 19, Annual Reviews, 493–530.

——, V. D. Larichev, J. C. McWilliams and G. M. Reznik, 1980: The dynamics of baroclinic and barotropic solitary eddies. *Dyn. Atmos. Oceans*, **5**, 1–41.

Haines, K., 1987a: Long lived eddies in planetary atmospheres. Ph.D. thesis. Imperial College, London, 232 pp.

——, 1987b: Solitary wave models of blocking persistence. Proc. NCAR Colloquium on Low Frequency Atmospheric Variability.

——, and J. C. Marshall, 1987: Eddy-forced coherent structures as a prototype of atmospheric blocking. *Quart. J. Roy. Meteor. Soc.*, **113**, 681–704.

Hoskins, B. J., and D. J. Karoly, 1981: The steady linear response of a spherical atmosphere to thermal and orographic forcing. *J. Atmos. Sci.*, **38**, 1179–1196.

——, I. N. James and G. H. White, 1983: The shape, propagation and mean-flow interaction of large-scale weather systems. *J. Atmos. Sci.*, **40**, 1595–1612.

——, M. E. McIntyre and A. W. Robertson, 1985: On the use and significance of isentropic potential vorticity maps. *Quart. J. Roy. Meteor. Soc.*, **111**, 877–946.

Illari, L., 1984: A diagnostic study of the potential vorticity in a warm blocking anti-cyclone. *J. Atmos. Sci.*, **41**, 3518–3526.

——, and J. C. Marshall, 1983: On the interpretation of eddy fluxes during a blocking episode. *J. Atmos. Sci.*, **40**, 2232–2242.

Leith, C. E., 1983: Predictability in theory and practice. *Large-Scale Dynamical Processes in the Atmosphere.* B. J. Hoskins and R. P. Pearce, Eds., Academic Press, 365–383.

——, 1984: Minimum enstrophy vortices. *Phys. Fluids*, **27**, 1388–1395.

Malanotte-Rizzoli, P., 1982: Planetary solitary waves in geophysical flows. *Advances in Geophysics*, Vol. 24, Academic Press, 147–224.

——, and P. J. Hancock, 1987: Coherent structures in a baroclinic atmosphere. Part IV: a comparison between theory and data. *J. Atmos. Sci.*, **44**, 2506–2529.

Malguzzi, P., and P. Malanotte-Rizzoli, 1984: Nonlinear stationary Rossby waves on non-uniform zonal winds and atmospheric blocking. Part I: The analytical theory. *J. Atmos. Sci.*, **41**, 2620–2628.

——, and ——, 1985: Coherent structures in a baroclinic atmosphere. Part II: A truncated model approach. *J. Atmos. Sci.*, **42**, 2463–2477.

Marshall, J. C., and G. Nurser, 1986: Steady, free circulation in a stratified quasi-geostrophic ocean. *J. Phys. Oceanogr.*, **16**, 1799–1813.

Matsuno, T., 1970: Vertical propagation of stationary planetary waves in the winter Northern Hemisphere. *J. Atmos. Sci.*, **27**, 871–883.

McWilliams, J. C., 1980: An application of equivalent modons to atmospheric blocking. *Dyn. Atmos. Oceans*, **5**, 43–66.

Pierrehumbert, R. T., and P. Malguzzi, 1984: Forced coherent structures and local multiple equilibria in a barotropic atmosphere. *J. Atmos. Sci.*, **41**, 246–257.

Read, P. L., P. B. Rhines and A. A. White, 1986: Geostrophic scatter diagrams and potential vorticity dynamics. *J. Atmos. Sci.*, **43**, 3226–3240.

Redekopp, L. G., 1977: On the theory of solitary Rossby waves. *J. Fluid Mech.*, **82**, 725–745.

Shutts, G. J., 1983: The propagation of eddies in diffluent jetstreams: Eddy vorticity forcing of "blocking" flow fields. *Quart. J. Roy. Meteor. Soc.*, **109**, 737–761.

——, 1986: A case study of eddy forcing during an Atlantic blocking episode. *Advances in Geophysics*, Vol. 29, Academic Press, 135–161.

Stern, M. E., 1975: Minimal properties of planetary eddies. *J. Mar. Res.*, **33**, 1–13.

Verkley, W. T. M., 1984: The construction of barotropic modons on a sphere. *J. Atmos. Sci.*, **41**, 2492–2504.

——, 1987: Stationary barotropic modons in westerly background flows. *J. Atmos. Sci.*, **44**, 2383–2398.

Whitham, G. B., 1974: *Linear and Nonlinear Waves.* Wiley, 636 pp.